EMDB	29779
PDB	8G6R
Microscope	Talos Arctica
Voltage (kV)	200
Detector	K3 direct electron detector (Gatan)
Dose Rate (e^-/pixel/sec)	12
Exposure Time (sec)	3.5
Electron Exposure ($e^-/Å^2$)	60
Frames (no.)	60
Defocus Values	-0.7 to -2.5
Sample Tilt (°)	25
Data Collection Mode	EFTEM, Counting, CDS
Nominal Magnification	105,000x
Pixel Size (Å)	0.834
Symmetry Imposed	C1
Movies Collected (no.)	1,261
Initial Particle Images (no.)	710,143
Final Particle Images (no.)	74,367
Map Resolution (Å) – GSFSC	3.3
Initial Model Used (PDB ID)	7CYQ
Non-hydrogen Atoms	9,410
Protein Residues	1075
Nuceic Acid Residues	40
R.M.S. Deviations	
Bond Lengths (Å)	0.004
Bond angles (°)	0.556
MolProbity Score	1.64
Clashscore	7.19
Ramachandran Plot	
Favored (%)	96.34
Allowed (%)	3.66
Disallowed (%)	0

Table S1: cryo-EM data collection and refinement. Information provided is for the cryo-EM data collection, and processing that produced the electron density map of the PEDV polymerase complex. Additionally, validation statistics for the polymerase complex coordinate model built into the reconstruction are provided.

	Desolvation Parameters	
Sample	**Capillary Temperature (°C)**	**In-source Trapping (V)**
PEDV nsp12+8+7	250	-150
PEDV A382R-nsp12+8+7	200	-300
PEDV V848R-nsp12+8+7	200	-200
PEDV nsp12+8+8L7	250	-300
SARS-CoV-2 nsp12+8+7	200	-150
SARS-CoV-2 L387R-nsp12+8+7	200	-150
SARS-CoV-2 T853R-nsp12+8+7	200	-160
SARS-CoV-2 nsp12+8+8L7	250	-150

Table S2, native mass spectrometry desolvation parameters: Parameters listed were optimized for each sample to remove as many adducts as possible without disrupting the complex(es) of interest.

Supplemental video 1, 3D variability analysis of PEDV core complex: The movie displays a series of 3D volumes (in gray) determined by 3D variability analysis (cryoSPARC v3.3.1). The movie begins by oscillating between the extremes of variability within the volume series. Docking our PEDV core complex model (nsp12 – light purple, nsp7 – green, nsp8 – red, primer – neon green, template – dark purple) into the densities reveals the flexibility of dsRNA leaving the active site. We predict that this movement results in the lack of complete reconstruction of our dsRNA and $nsp8_1$ N-terminal extension in our final map and model.

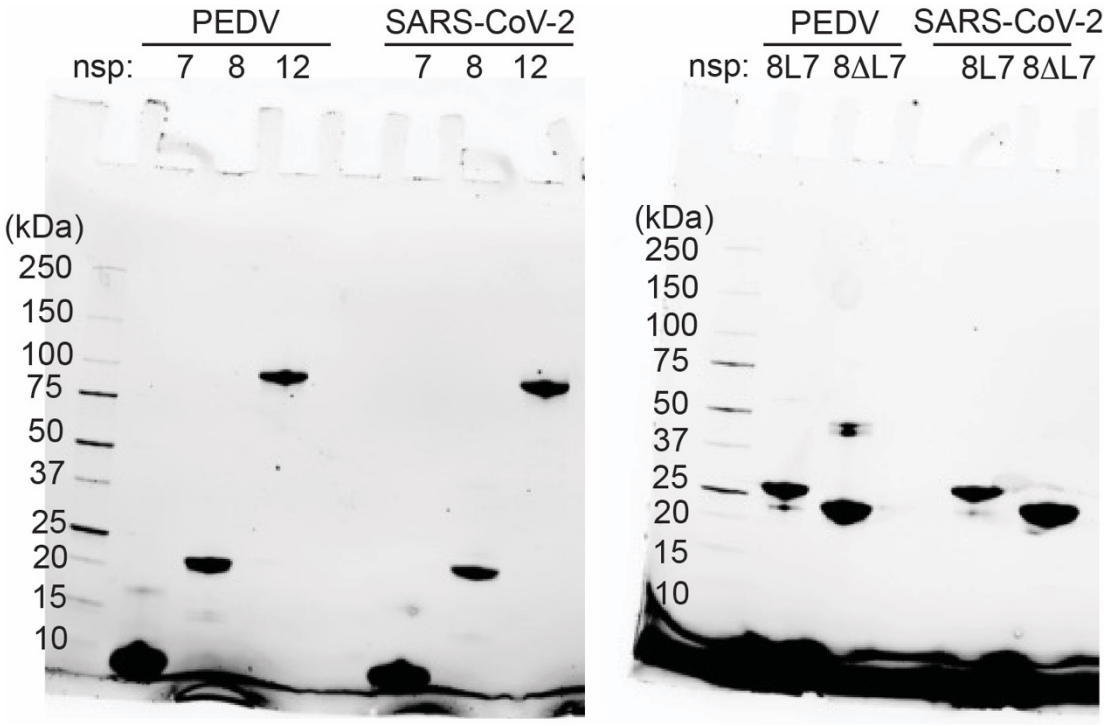

Figure S1, SDS-PAGE of viral proteins: Samples of purified proteins used for *in vitro* studies were run on pre-cast, stain-free, 4-20% SDS-PAGE gels (BioRad) and imaged using UV fluorescence. Expected molecular weights for different proteins are nsp7 – 9 kDa, nsp8 – 22 kDa, nsp12 – 110 kDa, nsp8L7 – 31 kDa, and nsp8ΔL7 – 25 kDa. The far-left lane of each gel is a protein ladder protein MWs labeled.

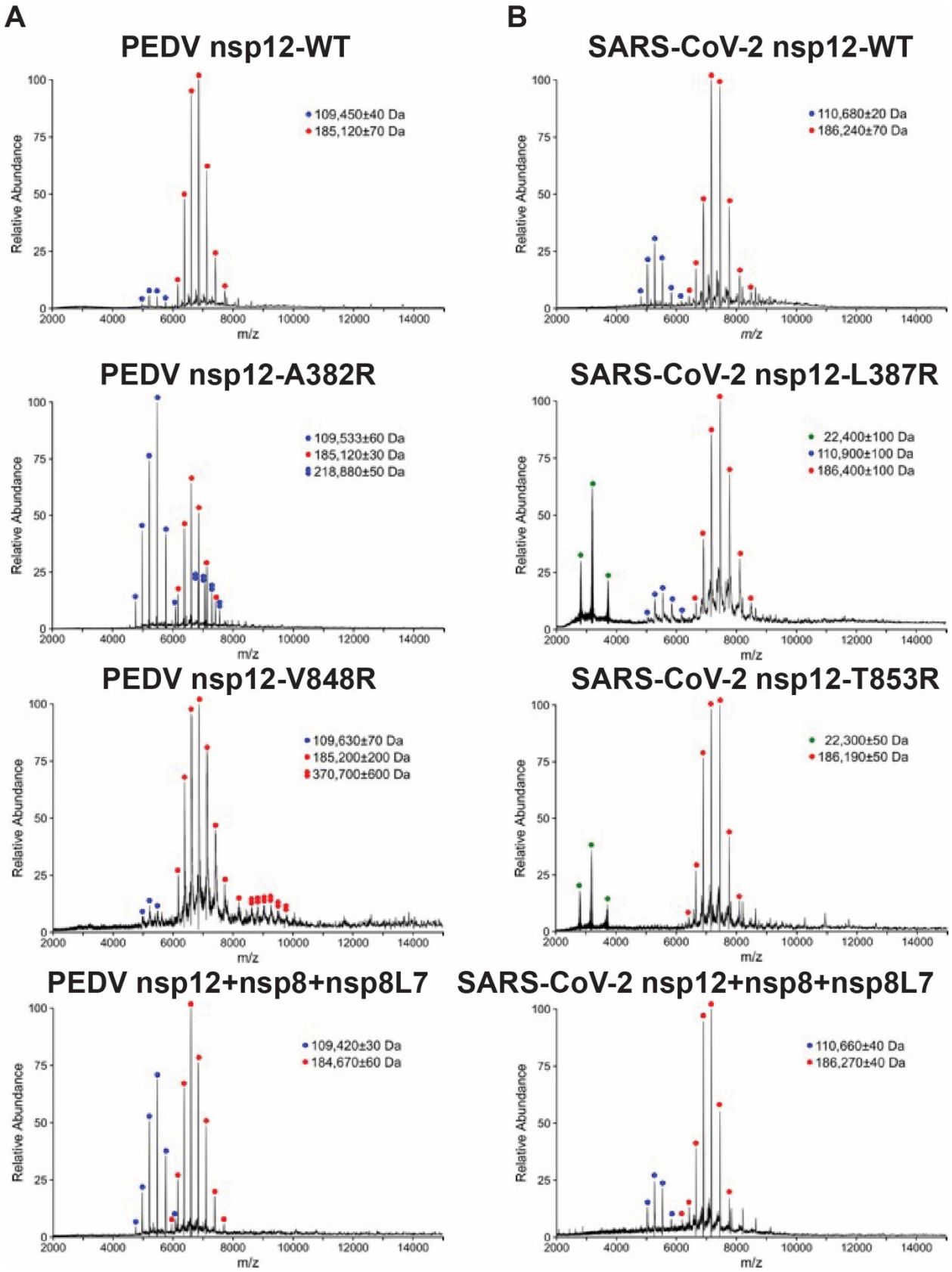

Figure S2, native mass spectrometry of coronavirus polymerase complexes. Native mass spectra for all coronavirus polymerase complexes tested with major mass populations labelled for each. Single and double red dots are monomeric and dimeric full intact complexes, respectively. Single and double blue dots are monomeric and dimeric solo nsp12, respectively. Green dots are free nsp8. **A)** SARS-CoV-2 complexes, top to

bottom: wildtype, L387R, T853R, nsp8L7. **B)** PEDV complexes, top to bottom: wildtype, A382R, V848R, nsp8L7.

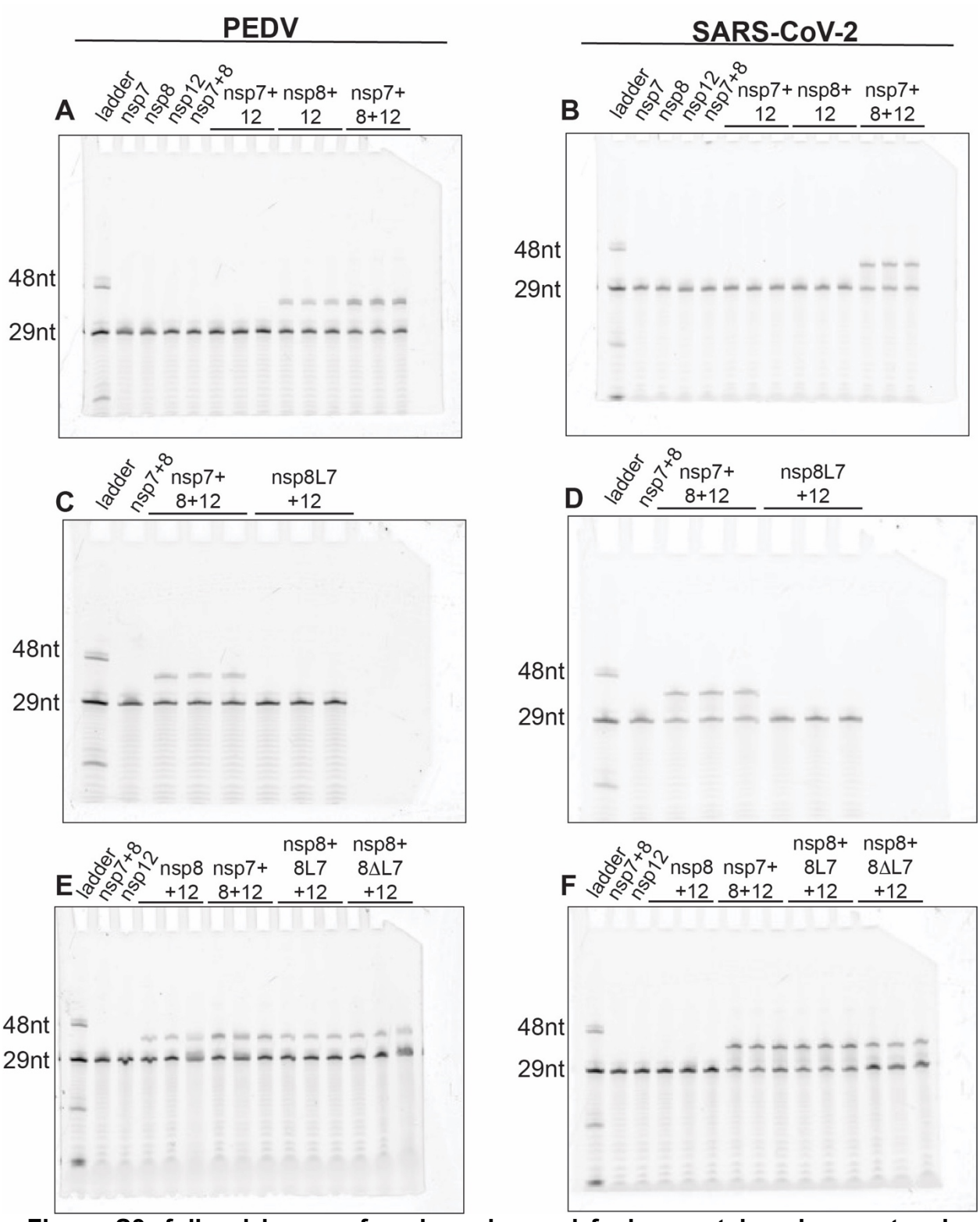

Figure S3, full gel images for piecewise and fusion protein primer extensions: Primer extensions assess the activity of nsp12 by its ability to extend an RNA primer (29 nucleotides or nt) to the length of its RNA template (38 nt) pair. **A)** PEDV piecewise primer extension revealing optimal nsp12 activity in the presence of both nsp7 and nsp8, and reduced activity with just nsp8. **B)** SARS2 piecewise primer extensions showing nsp12 is only active in the presence of both cofactors. Nsp8L7 does not individually activate nsp12 (**C** is PEDV, **D** is SARS-CoV-2). Nsp8L7 and nsp8ΔL7 activate nsp12 with free nsp8 present (**E** is PEDV, **F** is SARS-CoV-2), indicating polymerase activities requirement for $nsp8_1$, while $nsp8_2$'s helical extension is not essential for activity.

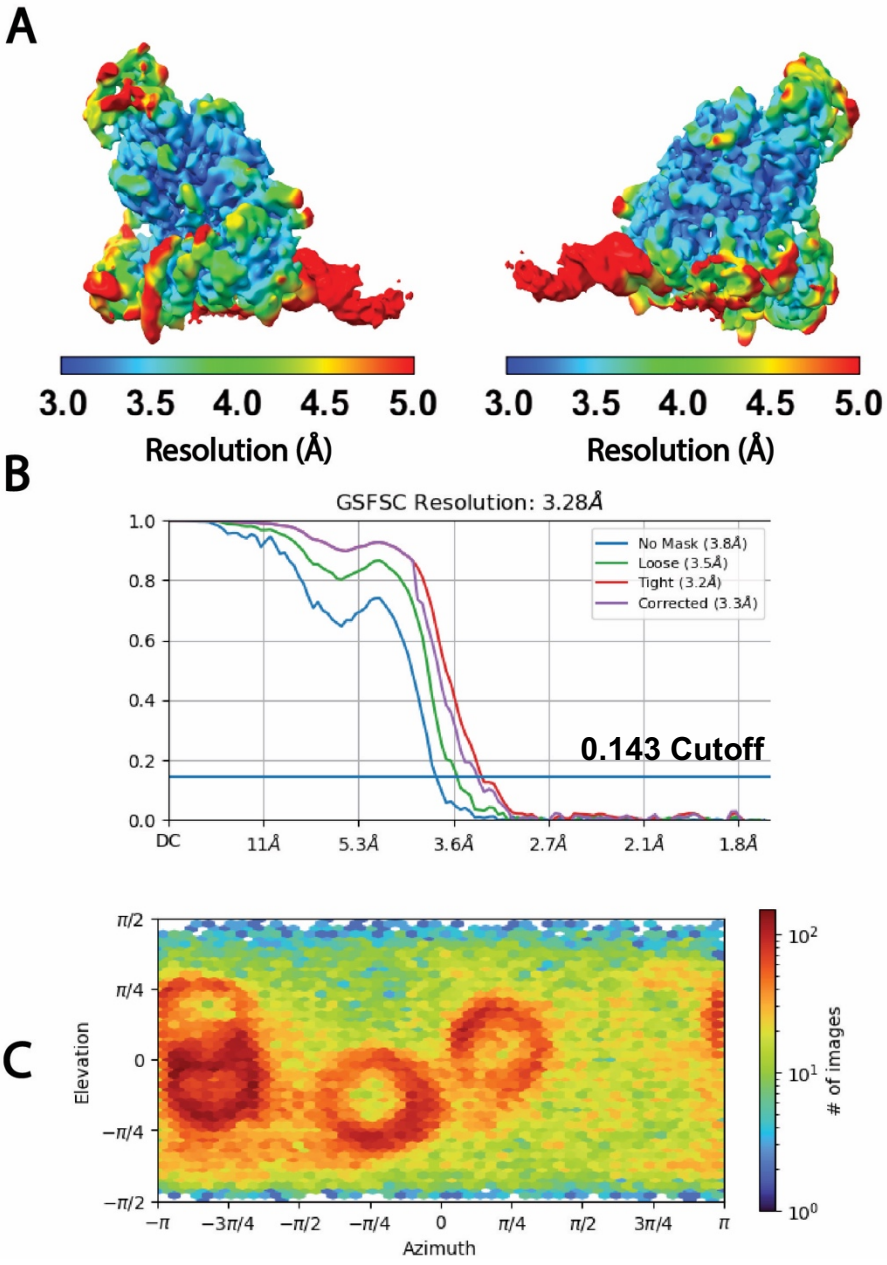

Figure S4, cryo-EM validation: A) Cryo-EM reconstruction filtered by local resolution according to the color key. B) Gold-standard Fourier shell correlation plot determined in cryoSPARC. The solid blue line marks the 0.143 cutoff. C) Particle orientation distribution plot for the final reconstruction. "# of images" indicates number of projections at a particular orientation (Elevation x Azimuth).

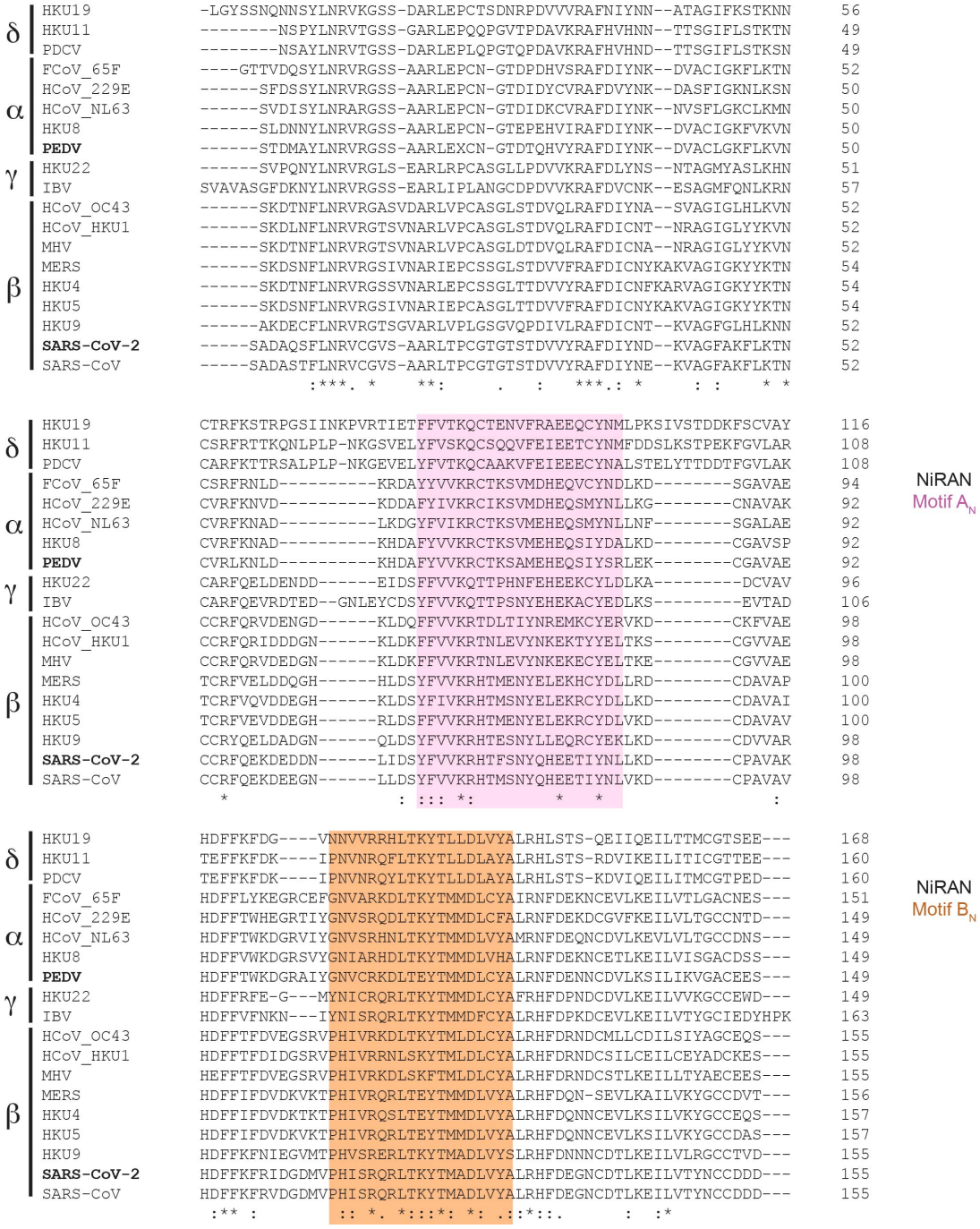
δ
α
γ
β
HKU19 -LGYSSNQNNSYLNRVKGSS-DARLEPCTSDNRPDVVVRAFNIYNN--ATAGIFKSTKNN 56
HKU11 --------NSPYLNRVTGSS-GARLEPQQPGVTPDAVKRAFHVHNN--TTSGIFLSTKTN 49
PDCV --------NSAYLNRVTGSS-DARLEPLQPGTQPDAVKRAFHVHND--TTSGIFLSTKSN 49
FCoV_65F ----GTTVDQSYLNRVRGSS-AARLEPCN-GTDPDHVSRAFDIYNK--DVACIGKFLKTN 52
HCoV_229E ------SFDSSYLNRVRGSS-AARLEPCN-GTDIDYCVRAFDVYNK--DASFIGKNLKSN 50
HCoV_NL63 ------SVDISYLNRARGSS-AARLEPCN-GTDIDKCVRAFDIYNK--NVSFLGKCLKMN 50
HKU8 ------SLDNNYLNRVRGSS-AARLEPCN-GTEPEHVIRAFDIYNK--DVACIGKFVKVN 50
PEDV ------STDMAYLNRVRGSS-AARLEXCN-GTDTQHVYRAFDIYNK--DVACLGKFLKVN 50
HKU22 ------SVPQNYLNRVRGLS-EARLRPCASGLLPDVVKRAFDLYNS--NTAGMYASLKHN 51
IBV SVAVASGFDKNYLNRVRGSS-EARLIPLANGCDPDVVKRAFDVCNK--ESAGMFQNLKRN 57
HCoV_OC43 ------SKDTNFLNRVRGASVDARLVPCASGLSTDVQLRAFDIYNA--SVAGIGLHLKVN 52
HCoV_HKU1 ------SKDLNFLNRVRGTSVNARLVPCASGLSTDVQLRAFDICNT--NRAGIGLYYKVN 52
MHV ------SKDTNFLNRVRGTSVNARLVPCASGLDTDVQLRAFDICNA--NRAGIGLYYKVN 52
MERS ------SKDSNFLNRVRGSIVNARIEPCSSGLSTDVVFRAFDICNYKAKVAGIGKYYKTN 54
HKU4 ------SKDTNFLNRVRGSSVNARLEPCSSGLTTDVVYRAFDICNFKARVAGIGKYYKTN 54
HKU5 ------SKDSNFLNRVRGSIVNARIEPCASGLTTDVVFRAFDICNYKAKVAGIGKYYKTN 54
HKU9 ------AKDECFLNRVRGTSGVARLVPLGSGVQPDIVLRAFDICNT--KVAGFGLHLKNN 52
SARS-CoV-2 -----SADAQSFLNRVCGVS-AARLTPCGTGTSTDVVYRAFDIYND--KVAGFAKFLKTN 52
SARS-CoV -----SADASTFLNRVCGVS-AARLTPCGTGTSTDVVYRAFDIYNE--KVAGFAKFLKTN 52
:***. * **: . : ***.: * : : * *
HKU19 CTRFKSTRPGSIINKPVRTIETFFVTKQCTENVFRAEEQCYNMLPKSIVSTDDKFSCVAY 116
HKU11 CSRFRTTKQNLPLP-NKGSVELYFVSKQCSQQVFEIEETCYNMFDDSLKSTPEKFGVLAR 108
PDCV CARFKTTRSALPLP-NKGEVELYFVTKQCAAKVFEIEEECYNALSTELYTTDDTFGVLAK 108
FCoV_65F CSRFRNLD----------KRDAYYVVKRCTKSVMDHEQVCYNDLKD--------SGAVAE 94
HCoV_229E CVRFKNVD----------KDDAFYIVKRCIKSVMDHEQSMYNLLKG--------CNAVAK 92
HCoV_NL63 CVRFKNAD----------LKDGYFVIKRCTKSVMEHEQSMYNLLNF--------SGALAE 92
HKU8 CVRFKNAD----------KHDAFYVVKRCTKSVMEHEQSIYDALKD--------CGAVSP 92
PEDV CVRLKNLD----------KHDAFYVVKRCTKSAMEHEQSIYSRLEK--------CGAVAE 92
HKU22 CARFQELDENDD------EIDSFFVVKQTTPHNFEHEEKCYLDLKA---------DCVAV 96
IBV CARFQEVRDTED--GNLEYCDSYFVVKQTTPSNYEHEKACYEDLKS---------EVTAD 106
HCoV_OC43 CCRFQRVDENGD------KLDQFFVVKRTDLTIYNREMKCYERVKD--------CKFVAE 98
HCoV_HKU1 CCRFQRIDDDGN------KLDKFFVVKRTNLEVYNKEKTYYELTKS--------CGVVAE 98
MHV CCRFQRVDEDGN------KLDKFFVVKRTNLEVYNKEKECYELTKE--------CGVVAE 98
MERS TCRFVELDDQGH------HLDSYFVVKRHTMENYELEKHCYDLLRD--------CDAVAP 100
HKU4 TCRFVQVDDEGH------KLDSYFIVKRHTMSNYELEKRCYDLLKD--------CDAVAI 100
HKU5 TCRFVEVDDEGH------RLDSFFVVKRHTMENYELEKRCYDLVKD--------CDAVAV 100
HKU9 CCRYQELDADGN------QLDSYFVVKRHTESNYLLEQRCYEKLKD--------CDVVAR 98
SARS-CoV-2 CCRFQEKDEDDN------LIDSYFVVKRHTFSNYQHEETIYNLLKD--------CPAVAK 98
SARS-CoV CCRFQEKDEEGN------LLDSYFVVKRHTMSNYQHEETIYNLVKD--------CPAVAV 98
* : ::: *: * * :
NiRAN
Motif A_N
HKU19 HDFFKFDG----VNNVVRRHLTKYTLLDLVYALRHLSTS-QEIIQEILTTMCGTSEE--- 168
HKU11 TEFFKFDK----IPNVNRQFLTKYTLLDLAYALRHLSTS-RDVIKEILITICGTTEE--- 160
PDCV TEFFKFDK----IPNVNRQYLTKYTLLDLAYALRHLSTS-KDVIQEILITMCGTPED--- 160
FCoV_65F HDFFLYKEGRCEFGNVARKDLTKYTMMDLCYAIRNFDEKNCEVLKEILVTLGACNES--- 151
HCoV_229E HDFFTWHEGRTIYGNVSRQDLTKYTMMDLCFALRNFDEKDCGVFKEILVLTGCCNTD--- 149
HCoV_NL63 HDFFTWKDGRVIYGNVSRHNLTKYTMMDLVYAMRNFDEQNCDVLKEVLVLTGCCDNS--- 149
HKU8 HDFFVWKDGRSVYGNIARHDLTKYTMMDLVHALRNFDEKNCETLKEILVISGACDSS--- 149
PEDV HDFFTWKDGRAIYGNVCRKDLTEYTMMDLCYALRNFDENNCDVLKSILIKVGACEES--- 149
HKU22 HDFFRFE-G---MYNICRQRLTKYTMMDLCYAFRHFDPNDCDVLKEILVVKGCCEWD--- 149
IBV HDFFVFNKN---IYNISRQRLTKYTMMDFCYALRHFDPKDCEVLKEILVTYGCIEDYHPK 163
HCoV_OC43 HDFFTFDVEGSRVPHIVRKDLTKYTMLDLCYALRHFDRNDCMLLCDILSIYAGCEQS--- 155
HCoV_HKU1 HDFFTFDIDGSRVPHIVRRNLSKYTMLDLCYALRHFDRNDCSILCEILCEYADCKES--- 155
MHV HEFFTFDVEGSRVPHIVRKDLSKFTMLDLCYALRHFDRNDCSTLKEILLTYAECEES--- 155
MERS HDFFIFDVDKVKTPHIVRQRLTEYTMMDLVYALRHFDQN-SEVLKAILVKYGCCDVT--- 156
HKU4 HDFFIFDVDKTKTPHIVRQSLTEYTMMDLVYALRHFDQNNCEVLKSILVKYGCCEQS--- 157
HKU5 HDFFIFDVDKVKTPHIVRQRLTEYTMMDLVYALRHFDQNNCEVLKSILVKYGCCDAS--- 157
HKU9 HDFFKFNIEGVMTPHVSRERLTKYTMADLVYSLRHFDNNNCDTLKEILVLRGCCTVD--- 155
SARS-CoV-2 HDFFKFRIDGDMVPHISRQRLTKYTMADLVYALRHFDEGNCDTLKEILVTYNCCDDD--- 155
SARS-CoV HDFFKFRVDGDMVPHISRQRLTKYTMADLVYALRHFDEGNCDTLKEILVTYNCCDDD--- 155
:** : :: *. *:::*: *: .:*::. : :*
NiRAN
Motif B_N

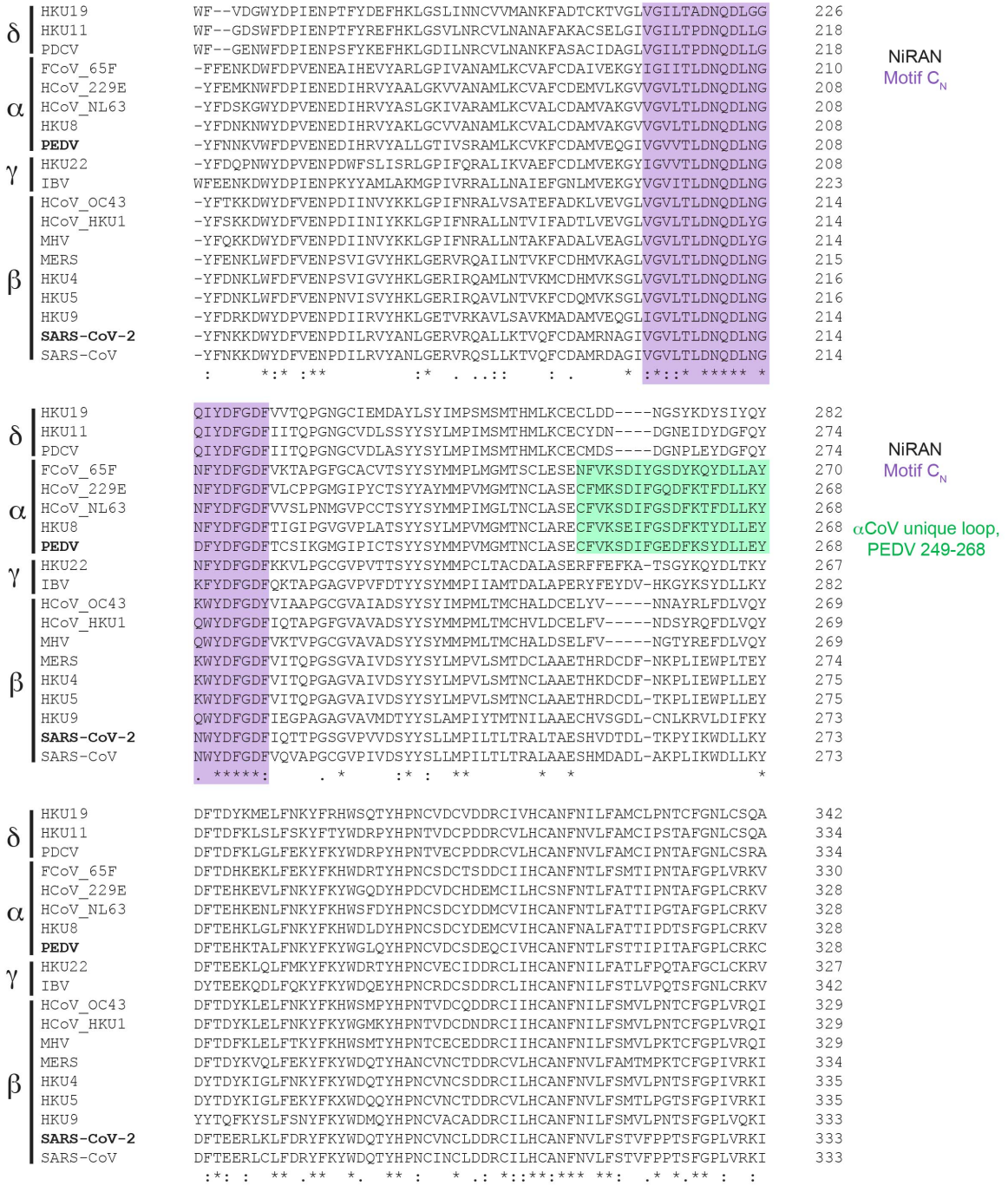
δ
α
γ
β
HKU19 WF--VDGWYDPIENPTFYDEFHKLGSLINNCVVMANKFADTCKTVGLVGILTADNQDLGG 226
HKU11 WF--GDSWFDPIENPTFYREFHKLGSVLNRCVLNANAFAKACSELGIVGILTPDNQDLLG 218
PDCV WF--GENWFDPIENPSFYKEFHKLGDILNRCVLNANKFASACIDAGLVGILTPDNQDLLG 218
FCoV_65F -FFENKDWFDPVENEAIHEVYARLGPIVANAMLKCVAFCDAIVEKGYIGIITLDNQDLNG 210
HCoV_229E -YFEMKNWFDPIENEDIHRVYAALGKVVANAMLKCVAFCDEMVLKGVVGVLTLDNQDLNG 208
HCoV_NL63 -YFDSKGWYDPVENEDIHRVYASLGKIVARAMLKCVALCDAMVAKGVVGVLTLDNQDLNG 208
HKU8 -YFDNKNWYDPVENEDIHRVYAKLGCVVANAMLKCVALCDAMVAKGVVGVLTLDNQDLNG 208
PEDV -YFNNKVWFDPVENEDIHRVYALLGTIVSRAMLKCVKFCDAMVEQGIVGVVTLDNQDLNG 208
HKU22 -YFDQPNWYDPVENPDWFSLISRLGPIFQRALIKVAEFCDLMVEKGYIGVVTLDNQDLNG 208
IBV WFEENKDWYDPIENPKYYAMLAKMGPIVRRALLNAIEFGNLMVEKGYVGVITLDNQDLNG 223
HCoV_OC43 -YFTKKDWYDFVENPDIINVYKKLGPIFNRALVSATEFADKLVEVGLVGVLTLDNQDLNG 214
HCoV_HKU1 -YFSKKDWYDFVENPDIINIYKKLGPIFNRALLNTVIFADTLVEVGLVGVLTLDNQDLYG 214
MHV -YFQKKDWYDFVENPDIINVYKKLGPIFNRALLNTAKFADALVEAGLVGVLTLDNQDLYG 214
MERS -YFENKLWFDFVENPSVIGVYHKLGERVRQAILNTVKFCDHMVKAGLVGVLTLDNQDLNG 215
HKU4 -YFDNKLWFDFVENPSVIGVYHKLGERIRQAMLNTVKMCDHMVKSGLVGVLTLDNQDLNG 216
HKU5 -YFDNKLWFDFVENPNVISVYHKLGERIRQAVLNTVKFCDQMVKSGLVGVLTLDNQDLNG 216
HKU9 -YFDRKDWYDPVENPDIIRVYHKLGETVRKAVLSAVKMADAMVEQGLIGVLTLDNQDLNG 214
SARS-CoV-2 -YFNKKDWYDFVENPDILRVYANLGERVRQALLKTVQFCDAMRNAGIVGVLTLDNQDLNG 214
SARS-CoV -YFNKKDWYDFVENPDILRVYANLGERVRQSLLKTVQFCDAMRDAGIVGVLTLDNQDLNG 214
NiRAN
Motif C_N
HKU19 QIYDFGDFVVTQPGNGCIEMDAYLSYIMPSMSMTHMLKCECLDD----NGSYKDYSIYQY 282
HKU11 QIYDFGDFIITQPGNGCVDLSSYYSYLMPIMSMTHMLKCECYDN----DGNEIDYDGFQY 274
PDCV QIYDFGDFIITQPGNGCVDLASYYSYLMPIMSMTHMLKCECMDS----DGNPLEYDGFQY 274
FCoV_65F NFYDFGDFVKTAPGFGCACVTSYYSYMMPLMGMTSCLESENFVKSDIYGSDYKQYDLLAY 270
HCoV_229E NFYDFGDFVLCPPGMGIPYCTSYYAYMMPVMGMTNCLASECFMKSDIFGQDFKTFDLLKY 268
HCoV_NL63 NFYDFGDFVVSLPNMGVPCCTSYYSYMMPIMGLTNCLASECFVKSDIFGSDFKTFDLLKY 268
HKU8 NFYDFGDFTIGIPGVGVPLATSYYSYLMPVMGMTNCLARECFVKSEIFGSDFKTYDLLEY 268
PEDV DFYDFGDFTCSIKGMGIPICTSYYSYMMPVMGMTNCLASECFVKSDIFGEDFKSYDLLEY 268
HKU22 NFYDFGDFKKVLPGCGVPVTTSYYSYMMPCLTACDALASERFFEFKA-TSGYKQYDLTKY 267
IBV KFYDFGDFQKTAPGAGVPVFDTYYSYMMPIIAMTDALAPERYFEYDV-HKGYKSYDLLKY 282
HCoV_OC43 KWYDFGDYVIAAPGCGVAIADSYYSYIMPMLTMCHALDCELYV-----NNAYRLFDLVQY 269
HCoV_HKU1 QWYDFGDFIQTAPGFGVAVADSYYSYMMPMLTMCHVLDCELFV-----NDSYRQFDLVQY 269
MHV QWYDFGDFVKTVPGCGVAVADSYYSYMMPMLTMCHALDSELFV-----NGTYREFDLVQY 269
MERS KWYDFGDFVITQPGSGVAIVDSYYSYLMPVLSMTDCLAAETHRDCDF-NKPLIEWPLTEY 274
HKU4 KWYDFGDFVITQPGAGVAIVDSYYSYLMPVLSMTNCLAAETHKDCDF-NKPLIEWPLLEY 275
HKU5 KWYDFGDFVITQPGAGVAIVDSYYSYLMPVLSMTNCLAAETHRDCDL-TKPLIEWPLLEY 275
HKU9 QWYDFGDFIEGPAGAGVAVMDTYYSLAMPIYTMTNILAAECHVSGDL-CNLKRVLDIFKY 273
SARS-CoV-2 NWYDFGDFIQTTPGSGVPVVDSYYSLLMPILTLTRALTAESHVDTDL-TKPYIKWDLLKY 273
SARS-CoV NWYDFGDFVQVAPGCGVPIVDSYYSLLMPILTLTRALAAESHMDADL-AKPLIKWDLLKY 273
NiRAN
Motif C_N
αCoV unique loop,
PEDV 249-268
HKU19 DFTDYKMELFNKYFRHWSQTYHPNCVDCVDDRCIVHCANFNILFAMCLPNTCFGNLCSQA 342
HKU11 DFTDFKLSLFSKYFTYWDRPYHPNTVDCPDDRCVLHCANFNVLFAMCIPSTAFGNLCSQA 334
PDCV DFTDFKLGLFEKYFKYWDRPYHPNTVECPDDRCVLHCANFNVLFAMCIPNTAFGNLCSRA 334
FCoV_65F DFTDHKEKLFEKYFKHWDRTYHPNCSDCTSDDCIIHCANFNTLFSMTIPNTAFGPLVRKV 330
HCoV_229E DFTEHKEVLFNKYFKYWGQDYHPDCVDCHDEMCILHCSNFNTLFATTIPNTAFGPLCRKV 328
HCoV_NL63 DFTEHKENLFNKYFKHWSFDYHPNCSDCYDDMCVIHCANFNTLFATTIPGTAFGPLCRKV 328
HKU8 DFTEHKLGLFNKYFKHWDLDYHPNCSDCYDEMCVIHCANFNALFATTIPDTSFGPLCRKV 328
PEDV DFTEHKTALFNKYFKYWGLQYHPNCVDCSDEQCIVHCANFNTLFSTTIPITAFGPLCRKC 328
HKU22 DFTEEKLQLFMKYFKYWDRTYHPNCVECIDDRCLIHCANFNILFATLFPQTAFGCLCKRV 327
IBV DYTEEKQDLFQKYFKYWDQEYHPNCRDCSDDRCLIHCANFNILFSTLVPQTSFGNLCRKV 342
HCoV_OC43 DFTDYKLELFNKYFKHWSMPYHPNTVDCQDDRCIIHCANFNILFSMVLPNTCFGPLVRQI 329
HCoV_HKU1 DFTDYKLELFNKYFKYWGMKYHPNTVDCDNDRCIIHCANFNILFSMVLPNTCFGPLVRQI 329
MHV DFTDFKLELFTKYFKHWSMTYHPNTCECEDDRCIIHCANFNILFSMVLPKTCFGPLVRQI 329
MERS DFTDYKVQLFEKYFKYWDQTYHANCVNCTDDRCVLHCANFNVLFAMTMPKTCFGPIVRKI 334
HKU4 DYTDYKIGLFNKYFKYWDQTYHPNCVNCSDDRCILHCANFNVLFSMVLPNTSFGPIVRKI 335
HKU5 DYTDYKIGLFEKYFKXWDQQYHPNCVNCTDDRCVLHCANFNVLFSMTLPGTSFGPIVRKI 335
HKU9 YYTQFKYSLFSNYFKYWDMQYHPNCVACADDRCILHCANFNILFSMVLPNTSFGPLVQKI 333
SARS-CoV-2 DFTEERLKLFDRYFKYWDQTYHPNCVNCLDDRCILHCANFNVLFSTVFPPTSFGPLVRKI 333
SARS-CoV DFTEERLCLFDRYFKYWDQTYHPNCINCLDDRCILHCANFNVLFSTVFPPTSFGPLVRKI 333

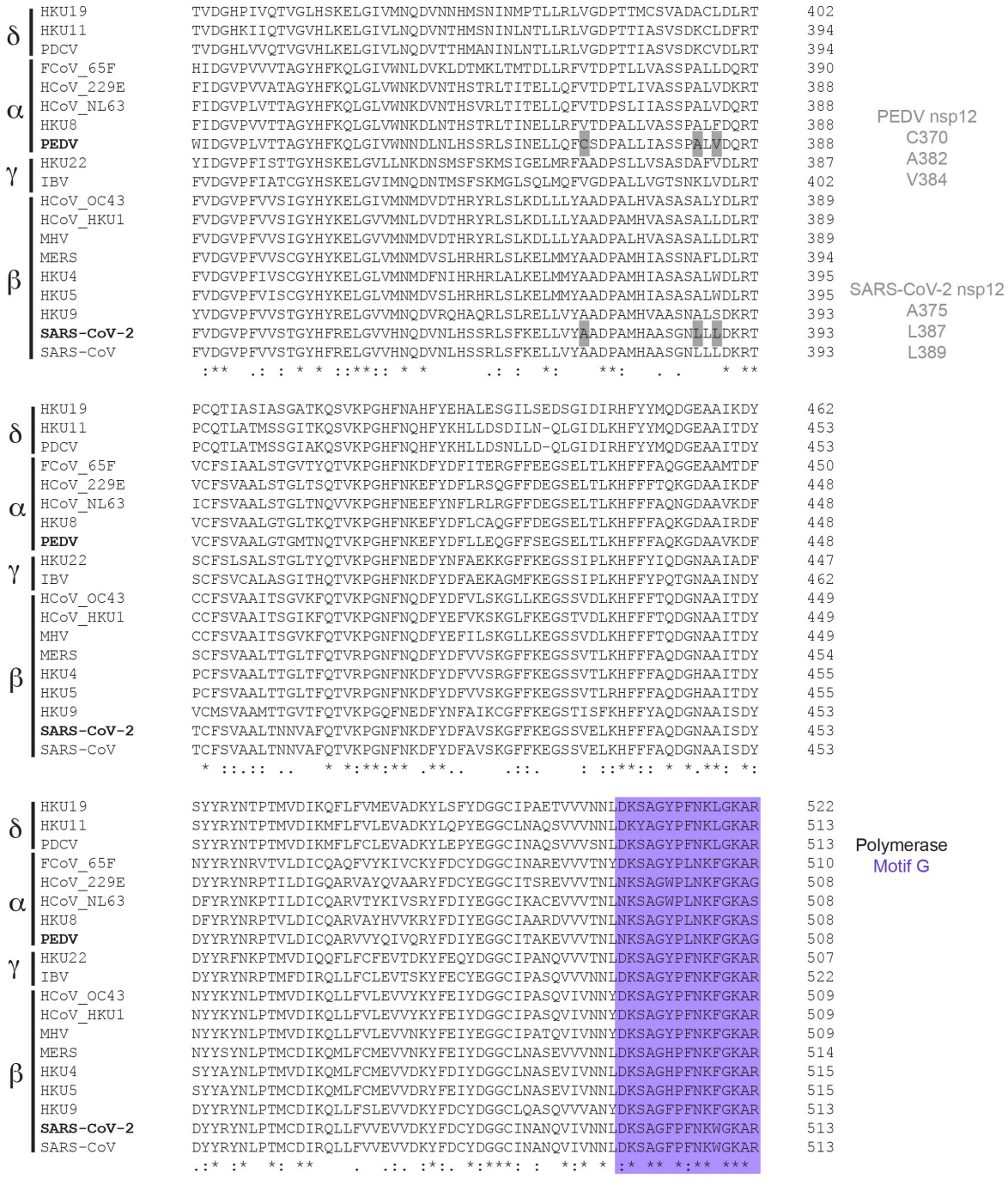
δ
α
γ
β
HKU19 TVDGHPIVQTVGLHSKELGIVMNQDVNNHMSNINMPTLLRLVGDPTTMCSVADACLDLRT 402
HKU11 TVDGHKIIQTVGVHLKELGIVLNQDVNTHMSNINLNTLLRLVGDPTTIASVSDKCLDFRT 394
PDCV TVDGHLVVQTVGVHLKELGIVLNQDVTTHMANINLNTLLRLVGDPTTIASVSDKCVDLRT 394
FCoV_65F HIDGVPVVVTAGYHFKQLGIVWNLDVKLDTMKLTMTDLLRFVTDPTLLVASSPALLDQRT 390
HCoV_229E FIDGVPVVATAGYHFKQLGLVWNKDVNTHSTRLTITELLQFVTDPTLIVASSPALVDKRT 388
HCoV_NL63 FIDGVPLVTTAGYHFKQLGLVWNKDVNTHSVRLTITELLQFVTDPSLIIASSPALVDQRT 388
HKU8 FIDGVPVVTTAGYHFKQLGLVWNKDLNTHSTRLTINELLRFVTDPALLVASSPALFDQRT 388
PEDV WIDGVPLVTTAGYHFKQLGIVWNNDLNLHSSRLSINELLQFCSDPALLIASSPALVDQRT 388
HKU22 YIDGVPFISTTGYHSKELGVLLNKDNSMSFSKMSIGELMRFAADPSLLVSASDAFVDLRT 387
IBV FVDGVPFIATCGYHSKELGVIMNQDNTMSFSKMGLSQLMQFVGDPALLVGTSNKLVDLRT 402
HCoV_OC43 FVDGVPFVVSIGYHYKELGIVMNMDVDTHRYRLSLKDLLLYAADPALHVASASALYDLRT 389
HCoV_HKU1 FVDGVPFVVSIGYHYKELGVVMNLDVDTHRYRLSLKDLLLYAADPAMHVASASALLDLRT 389
MHV FVDGVPFVVSIGYHYKELGVVMNMDVDTHRYRLSLKDLLLYAADPALHVASASALLDLRT 389
MERS FVDGVPFVVSCGYHYKELGLVMNMDVSLHRHRLSLKELMMYAADPAMHIASSNAFLDLRT 394
HKU4 FVDGVPFIVSCGYHYKELGLVMNMDFNIHRHRLALKELMMYAADPAMHIASASALWDLRT 395
HKU5 FVDGVPFVISCGYHYKELGLVMNMDVSLHRHRLSLKELMMYAADPAMHIASASALWDLRT 395
HKU9 YVDGVPFVVSTGYHYRELGVVMNQDVRQHAQRLSLRELLVYAADPAMHVAASNALSDKRT 393
SARS-CoV-2 FVDGVPFVVSTGYHFRELGVVHNQDVNLHSSRLSFKELLVYAADPAMHAASGNLLLDKRT 393
SARS-CoV FVDGVPFVVSTGYHFRELGVVHNQDVNLHSSRLSFKELLVYAADPAMHAASGNLLLDKRT 393
:** .: : * * ::**:: * * .: : *: **: . . * **
PEDV nsp12
C370
A382
V384
SARS-CoV-2 nsp12
A375
L387
L389
HKU19 PCQTIASIASGATKQSVKPGHFNAHFYEHALESGILSEDSGIDIRHFYYMQDGEAAIKDY 462
HKU11 PCQTLATMSSGITKQSVKPGHFNQHFYKHLLDSDILN-QLGIDLKHFYYMQDGEAAITDY 453
PDCV PCQTLATMSSGIAKQSVKPGHFNQHFYKHLLDSNLLD-QLGIDIRHFYYMQDGEAAITDY 453
FCoV_65F VCFSIAALSTGVTYQTVKPGHFNKDFYDFITERGFFEEGSELTLKHFFFAQGGEAAMTDF 450
HCoV_229E VCFSVAALSTGLTSQTVKPGHFNKEFYDFLRSQGFFDEGSELTLKHFFFTQKGDAAIKDF 448
HCoV_NL63 ICFSVAALSTGLTNQVVKPGHFNEEFYNFLRLRGFFDEGSELTLKHFFFAQNGDAAVKDF 448
HKU8 VCFSVAALGTGLTKQTVKPGHFNKEFYDFLCAQGFFDEGSELTLKHFFFAQKGDAAIRDF 448
PEDV VCFSVAALGTGMTNQTVKPGHFNKEFYDFLLEQGFFSEGSELTLKHFFFAQKGDAAVKDF 448
HKU22 SCFSLSALSTGLTYQTVKPGHFNEDFYNFAEKKGFFKEGSSIPLKHFFYIQDGNAAIADF 447
IBV SCFSVCALASGITHQTVKPGHFNKDFYDFAEKAGMFKEGSSIPLKHFFYPQTGNAAINDY 462
HCoV_OC43 CCFSVAAITSGVKFQTVKPGNFNQDFYDFVLSKGLLKEGSSVDLKHFFFTQDGNAAITDY 449
HCoV_HKU1 CCFSVAAITSGIKFQTVKPGNFNQDFYEFVKSKGLFKEGSTVDLKHFFFTQDGNAAITDY 449
MHV CCFSVAAITSGVKFQTVKPGNFNQDFYEFILSKGLLKEGSSVDLKHFFFTQDGNAAITDY 449
MERS SCFSVAALTTGLTFQTVRPGNFNQDFYDFVVSKGFFKEGSSVTLKHFFFAQDGNAAITDY 454
HKU4 PCFSVAALTTGLTFQTVRPGNFNKDFYDFVVSRGFFKEGSSVTLKHFFFAQDGHAAITDY 455
HKU5 PCFSVAALTTGLTFQTVRPGNFNKDFYDFVVSKGFFKEGSSVTLRHFFFAQDGHAAITDY 455
HKU9 VCMSVAAMTTGVTFQTVKPGQFNEDFYNFAIKCGFFKEGSTISFKHFFYAQDGNAAISDY 453
SARS-CoV-2 TCFSVAALTNNVAFQTVKPGNFNKDFYDFAVSKGFFKEGSSVELKHFFFAQDGNAAISDY 453
SARS-CoV TCFSVAALTNNVAFQTVKPGNFNKDFYDFAVSKGFFKEGSSVELKHFFFAQDGNAAISDY 453
* ::.:: .. * *:**:** .**.. .::. : ::**:: * *.**: *:
HKU19 SYYRYNTPTMVDIKQFLFVMEVADKYLSFYDGGCIPAETVVVNNLDKSAGYPFNKLGKAR 522
HKU11 SYYRYNTPTMVDIKMFLFVLEVADKYLQPYEGGCLNAQSVVVNNLDKYAGYPFNKLGKAR 513
PDCV SYYRYNTPTMVDIKMFLFCLEVADKYLEPYEGGCINAQSVVVSNLDKSAGYPFNKLGKAR 513
FCoV_65F NYYRYNRVTVLDICQAQFVYKIVCKYFDCYDGGCINAREVVVTNYDKSAGYPLNKFGKAR 510
HCoV_229E DYYRYNRPTILDIGQARVAYQVAARYFDCYEGGCITSREVVVTNLNKSAGWPLNKFGKAG 508
HCoV_NL63 DFYRYNKPTILDICQARVTYKIVSRYFDIYEGGCIKACEVVVTNLNKSAGWPLNKFGKAS 508
HKU8 DFYRYNRPTVLDICQARVAYHVVKRYFDIYEGGCIAARDVVVTNLNKSAGYPLNKFGKAS 508
PEDV DYYRYNRPTVLDICQARVVYQIVQRYFDIYEGGCITAKEVVVTNLNKSAGYPLNKFGKAG 508
HKU22 DYYRFNKPTMVDIQQFLFCFEVTDKYFEQYDGGCIPANQVVVTNLDKSAGYPFNKFGKAR 507
IBV DYYRYNRPTMFDIRQLLFCLEVTSKYFECYEGGCIPASQVVVNNLDKSAGYPFNKFGKAR 522
HCoV_OC43 NYYKYNLPTMVDIKQLLFVLEVVYKYFEIYDGGCIPASQVIVNNYDKSAGYPFNKFGKAR 509
HCoV_HKU1 NYYKYNLPTMVDIKQLLFVLEVVYKYFEIYDGGCIPASQVIVNNYDKSAGYPFNKFGKAR 509
MHV NYYKYNLPTMVDIKQLLFVLEVVNKYFEIYEGGCIPATQVIVNNYDKSAGYPFNKFGKAR 509
MERS NYYSYNLPTMCDIKQMLFCMEVVNKYFEIYDGGCLNASEVVVNNLDKSAGHPFNKFGKAR 514
HKU4 SYYAYNLPTMVDIKQMLFCMEVVDKYFDIYDGGCLNASEVIVNNLDKSAGHPFNKFGKAR 515
HKU5 SYYAYNLPTMCDIKQMLFCMEVVDRYFEIYDGGCLNASEVIVNNLDKSAGHPFNKFGKAR 515
HKU9 DYYRYNLPTMCDIKQLLFSLEVVDKYFDCYDGGCLQASQVVVANYDKSAGFPFNKFGKAR 513
SARS-CoV-2 DYYRYNLPTMCDIRQLLFVVEVVDKYFDCYDGGCINANQVIVNNLDKSAGFPFNKWGKAR 513
SARS-CoV DYYRYNLPTMCDIRQLLFVVEVVDKYFDCYDGGCINANQVIVNNLDKSAGFPFNKWGKAR 513
.:* :* *: ** . .:. :*:. *:***: : *:* * :* ** *:** ***
Polymerase
Motif G

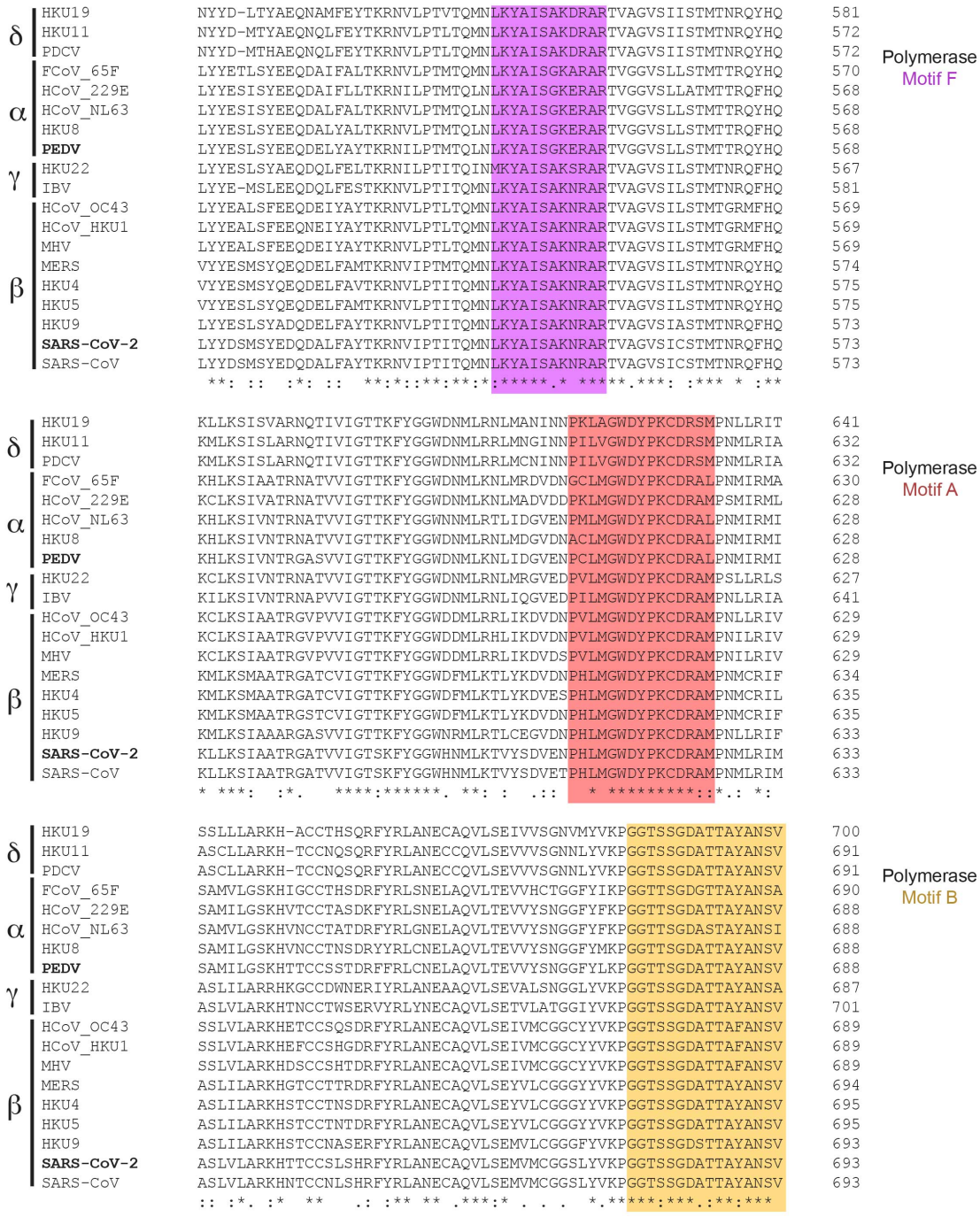
δ
α
γ
β
HKU19 NYYD-LTYAEQNAMFEYTKRNVLPTVTQMNLKYAISAKDRARTVAGVSIISTMTNRQYHQ 581
HKU11 NYYD-MTYAEQNQLFEYTKRNVLPTLTQMNLKYAISAKDRARTVAGVSIISTMTNRQYHQ 572
PDCV NYYD-MTHAEQNQLFEYTKRNVLPTLTQMNLKYAISAKDRARTVAGVSIISTMTNRQYHQ 572
FCoV_65F LYYETLSYEEQDAIFALTKRNVLPTMTQMNLKYAISGKARARTVGGVSLLSTMTTRQYHQ 570
HCoV_229E LYYESISYEEQDAIFLLTKRNILPTMTQLNLKYAISGKERARTVGGVSLLATMTTRQFHQ 568
HCoV_NL63 LYYESISYEEQDALFALTKRNVLPTMTQLNLKYAISGKERARTVGGVSLLSTMTTRQYHQ 568
HKU8 LYYESLSYEEQDALYALTKRNVLPTMTQLNLKYAISGKERARTVGGVSLLSTMTTRQFHQ 568
PEDV LYYESLSYEEQDELYAYTKRNILPTMTQLNLKYAISGKERARTVGGVSLLSTMTTRQYHQ 568
HKU22 LYYESLSYAEQDQLFELTKRNILPTITQINMKYAISAKSRARTVAGVSILSTMTNRQFHQ 567
IBV LYYE-MSLEEQDQLFESTKKNVLPTITQMNLKYAISAKNRARTVAGVSILSTMTNRQFHQ 581
HCoV_OC43 LYYEALSFEEQDEIYAYTKRNVLPTLTQMNLKYAISAKNRARTVAGVSILSTMTGRMFHQ 569
HCoV_HKU1 LYYEALSFEEQNEIYAYTKRNVLPTLTQMNLKYAISAKNRARTVAGVSILSTMTGRMFHQ 569
MHV LYYEALSFEEQDEIYAYTKRNVLPTLTQMNLKYAISAKNRARTVAGVSILSTMTGRMFHQ 569
MERS VYYESMSYQEQDELFAMTKRNVIPTMTQMNLKYAISAKNRARTVAGVSILSTMTNRQYHQ 574
HKU4 VYYESMSYQEQDELFAVTKRNVLPTITQMNLKYAISAKNRARTVAGVSILSTMTNRQYHQ 575
HKU5 VYYESLSYQEQDELFAMTKRNVLPTITQMNLKYAISAKNRARTVAGVSILSTMTNRQYHQ 575
HKU9 LYYESLSYADQDELFAYTKRNVLPTITQMNLKYAISAKNRARTVAGVSIASTMTNRQFHQ 573
SARS-CoV-2 LYYDSMSYEDQDALFAYTKRNVIPTITQMNLKYAISAKNRARTVAGVSICSTMTNRQFHQ 573
SARS-CoV LYYDSMSYEDQDALFAYTKRNVIPTITQMNLKYAISAKNRARTVAGVSICSTMTNRQFHQ 573
: :: :*: :: **:*:::**:*:*****.* ******.***: :*** * :**
Polymerase
Motif F
HKU19 KLLKSISVARNQTIVIGTTKFYGGWDNMLRNLMANINNPKLAGWDYPKCDRSMPNLLRIT 641
HKU11 KMLKSISLARNQTIVIGTTKFYGGWDNMLRRLMNGINNPILVGWDYPKCDRSMPNMLRIA 632
PDCV KMLKSISLARNQTIVIGTTKFYGGWDNMLRRLMCNINNPILVGWDYPKCDRSMPNMLRIA 632
FCoV_65F KHLKSIAATRNATVVIGTTKFYGGWDNMLKNLMRDVDNGCLMGWDYPKCDRALPNMIRMA 630
HCoV_229E KCLKSIVATRNATVVIGTTKFYGGWDNMLKNLMADVDDPKLMGWDYPKCDRAMPSMIRML 628
HCoV_NL63 KHLKSIVNTRNATVVIGTTKFYGGWNNMLRTLIDGVENPMLMGWDYPKCDRALPNMIRMI 628
HKU8 KHLKSIVNTRNATVVIGTTKFYGGWDNMLRNLMDGVDNACLMGWDYPKCDRALPNMIRMI 628
PEDV KHLKSIVNTRGASVVIGTTKFYGGWDNMLKNLIDGVENPCLMGWDYPKCDRALPNMIRMI 628
HKU22 KCLKSIVNTRNATVVIGTTKFYGGWDNMLRNLMRGVEDPVLMGWDYPKCDRAMPSLLRLS 627
IBV KILKSIVNTRNAPVVIGTTKFYGGWDNMLRNLIQGVEDPILMGWDYPKCDRAMPNLLRIA 641
HCoV_OC43 KCLKSIAATRGVPVVIGTTKFYGGWDDMLRRLIKDVDNPVLMGWDYPKCDRAMPNLLRIV 629
HCoV_HKU1 KCLKSIAATRGVPVVIGTTKFYGGWDDMLRHLIKDVDNPVLMGWDYPKCDRAMPNILRIV 629
MHV KCLKSIAATRGVPVVIGTTKFYGGWDDMLRRLIKDVDSPVLMGWDYPKCDRAMPNILRIV 629
MERS KMLKSMAATRGATCVIGTTKFYGGWDFMLKTLYKDVDNPHLMGWDYPKCDRAMPNMCRIF 634
HKU4 KMLKSMAATRGATCVIGTTKFYGGWDFMLKTLYKDVESPHLMGWDYPKCDRAMPNMCRIL 635
HKU5 KMLKSMAATRGSTCVIGTTKFYGGWDFMLKTLYKDVDNPHLMGWDYPKCDRAMPNMCRIF 635
HKU9 KMLKSIAAARGASVVIGTTKFYGGWNRMLRTLCEGVDNPHLMGWDYPKCDRAMPNLLRIF 633
SARS-CoV-2 KLLKSIAATRGATVVIGTSKFYGGWHNMLKTVYSDVENPHLMGWDYPKCDRAMPNMLRIM 633
SARS-CoV KLLKSIAATRGATVVIGTSKFYGGWHNMLKTVYSDVETPHLMGWDYPKCDRAMPNMLRIM 633
* ***: :*. ****:******. **: : .:: * *********::*.: *:
Polymerase
Motif A
HKU19 SSLLLARKH-ACCTHSQRFYRLANECAQVLSEIVVSGNVMYVKPGGTSSGDATTAYANSV 700
HKU11 ASCLLARKH-TCCNQSQRFYRLANECCQVLSEVVVSGNNLYVKPGGTSSGDATTAYANSV 691
PDCV ASCLLARKH-TCCNQSQRFYRLANECCQVLSEVVVSGNNLYVKPGGTSSGDATTAYANSV 691
FCoV_65F SAMVLGSKHIGCCTHSDRFYRLSNELAQVLTEVVHCTGGFYIKPGGTTSGDGTTAYANSA 690
HCoV_229E SAMILGSKHVTCCTASDKFYRLSNELAQVLTEVVYSNGGFYFKPGGTTSGDATTAYANSV 688
HCoV_NL63 SAMVLGSKHVNCCTATDRFYRLGNELAQVLTEVVYSNGGFYFKPGGTTSGDASTAYANSI 688
HKU8 SAMILGSKHVNCCTNSDRYYRLCNELAQVLTEVVYSNGGFYMKPGGTTSGDATTAYANSV 688
PEDV SAMILGSKHTTCCSSTDRFFRLCNELAQVLTEVVYSNGGFYLKPGGTTSGDATTAYANSV 688
HKU22 ASLILARRHKGCCDWNERIYRLANEAAQVLSEVALSNGGLYVKPGGTSSGDATTAYANSA 687
IBV ASLVLARKHTNCCTWSERVYRLYNECAQVLSETVLATGGIYVKPGGTSSGDATTAYANSV 701
HCoV_OC43 SSLVLARKHETCCSQSDRFYRLANECAQVLSEIVMCGGCYYVKPGGTSSGDATTAFANSV 689
HCoV_HKU1 SSLVLARKHEFCCSHGDRFYRLANECAQVLSEIVMCGGCYYVKPGGTSSGDATTAFANSV 689
MHV SSLVLARKHDSCCSHTDRFYRLANECAQVLSEIVMCGGCYYVKPGGTSSGDATTAFANSV 689
MERS ASLILARKHGTCCTTRDRFYRLANECAQVLSEYVLCGGGYYVKPGGTSSGDATTAYANSV 694
HKU4 ASLILARKHSTCCTNSDRFYRLANECAQVLSEYVLCGGGYYVKPGGTSSGDATTAYANSV 695
HKU5 ASLILARKHSTCCTNTDRFYRLANECAQVLSEYVLCGGGYYVKPGGTSSGDATTAYANSV 695
HKU9 ASLILARKHSTCCNASERFYRLANECAQVLSEMVLCGGGFYVKPGGTSSGDSTTAYANSV 693
SARS-CoV-2 ASLVLARKHTTCCSLSHRFYRLANECAQVLSEMVMCGGSLYVKPGGTSSGDATTAYANSV 693
SARS-CoV ASLVLARKHNTCCNLSHRFYRLANECAQVLSEMVMCGGSLYVKPGGTSSGDATTAYANSV 693
:: :*. :* ** .: :** ** .***:* . . . *.******:***.:**:***
Polymerase
Motif B

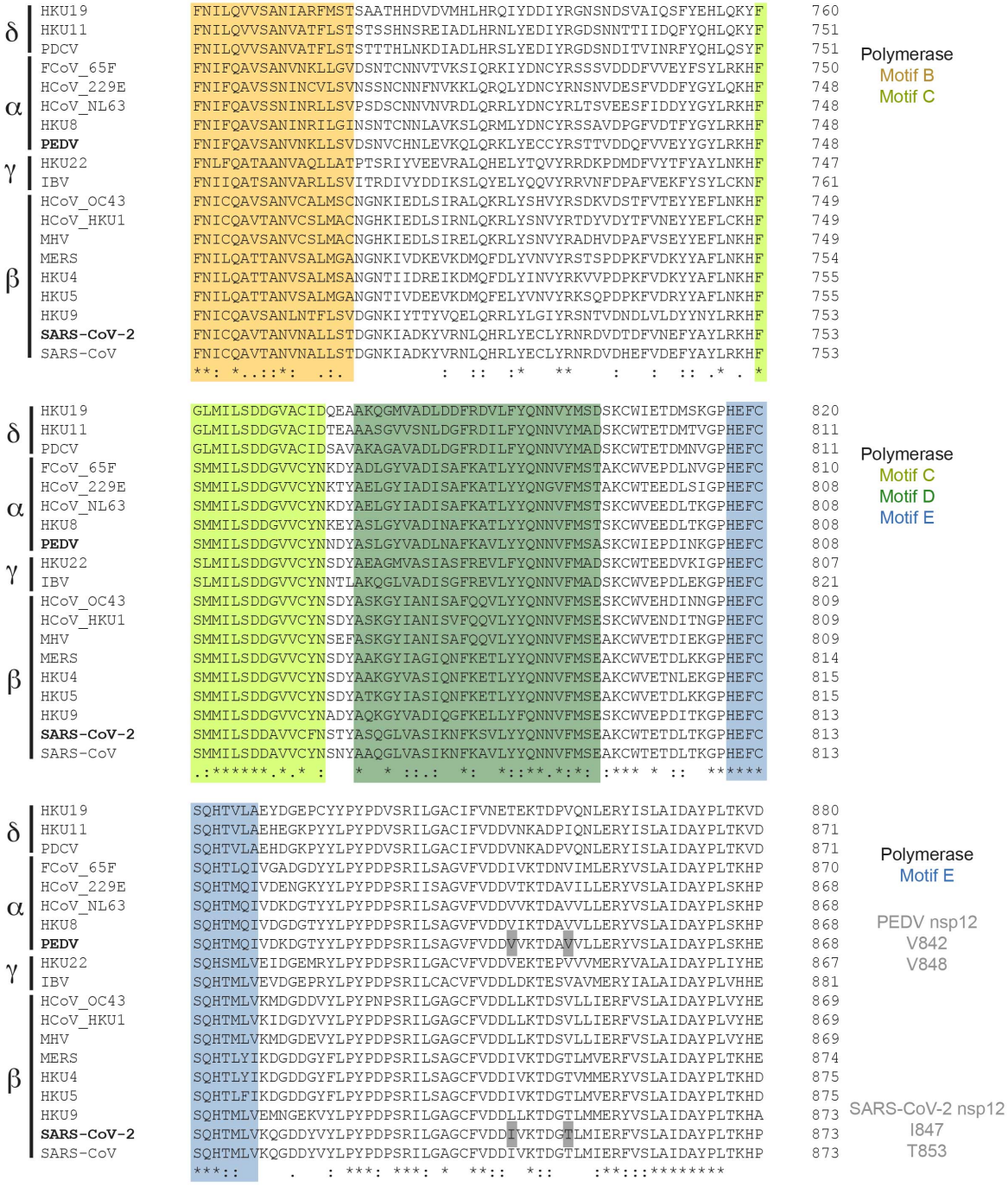
δ
α
γ
β
HKU19
HKU11
PDCV
FCoV_65F
HCoV_229E
HCoV_NL63
HKU8
PEDV
HKU22
IBV
HCoV_OC43
HCoV_HKU1
MHV
MERS
HKU4
HKU5
HKU9
SARS-CoV-2
SARS-CoV
760
751
751
750
748
748
748
748
747
761
749
749
749
754
755
755
753
753
753
Polymerase
Motif B
Motif C
820
811
811
810
808
808
808
808
807
821
809
809
809
814
815
815
813
813
813
Polymerase
Motif C
Motif D
Motif E
880
871
871
870
868
868
868
868
867
881
869
869
869
874
875
875
873
873
873
Polymerase
Motif E
PEDV nsp12
V842
V848
SARS-CoV-2 nsp12
I847
T853

Figure S5, Multiple sequence alignment of coronavirus nsp12s. Alignment of nsp12 from the alpha- (FCoV-65F, HCoV-229E, HCoV-NL63, HKU8, PEDV), beta- (HCoV-OC43, HKU1, MHV MERS, HKU4, HKU5, HKU9, SARS-CoV, SARS-CoV-2), gamma (HKU22, IBV), and delta- (HKU19, HKU11, PDCV) coronavirus genera. Global alignment was done using Clustal Omega [2]. Residues marked with "*" are conserved, ":" are very similar, and "." are moderately similar residues.

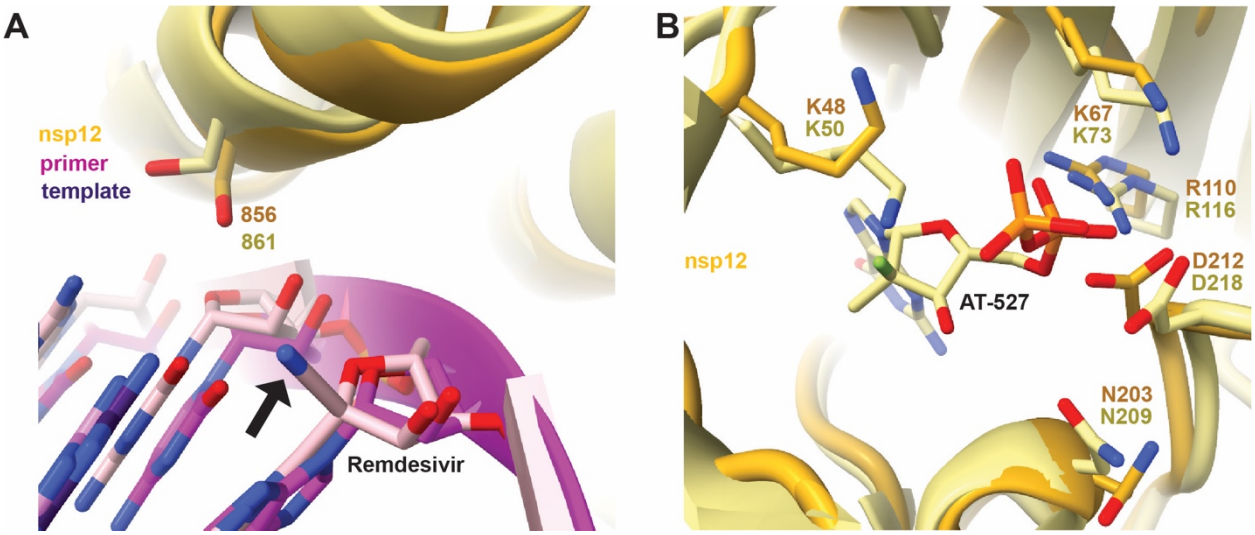

Figure S6: possible cross-effectiveness of CoV antivirals. In each figure PEDV nsp12 is shown in dark yellow and the RNA primer in dark pink, superimposed are SARS-CoV-2 models in lighter, matching colors. **A)** The antiviral Remdesivir's 1'-cyano group (black arrow) is believed to clash with SARS-CoV-2 nsp12 S861 in the +4 extension position. Remdesivir incorporated into a nascent primer at +3 is shown (PDB ID: 7B3C). Due to the sequence and spatial homology of S856 in PEDV we predict Remdesivir would have similar effectiveness against PEDV. **B**) The dual action antiviral AT-527 was shown to bind and inhibit the NiRAN domain of SARS-CoV-2 nsp12 (PDB ID: 7ED5). Several residues important for drug binding are conserved in PEDV, shown are K48, K67, R110, N203, and D212.

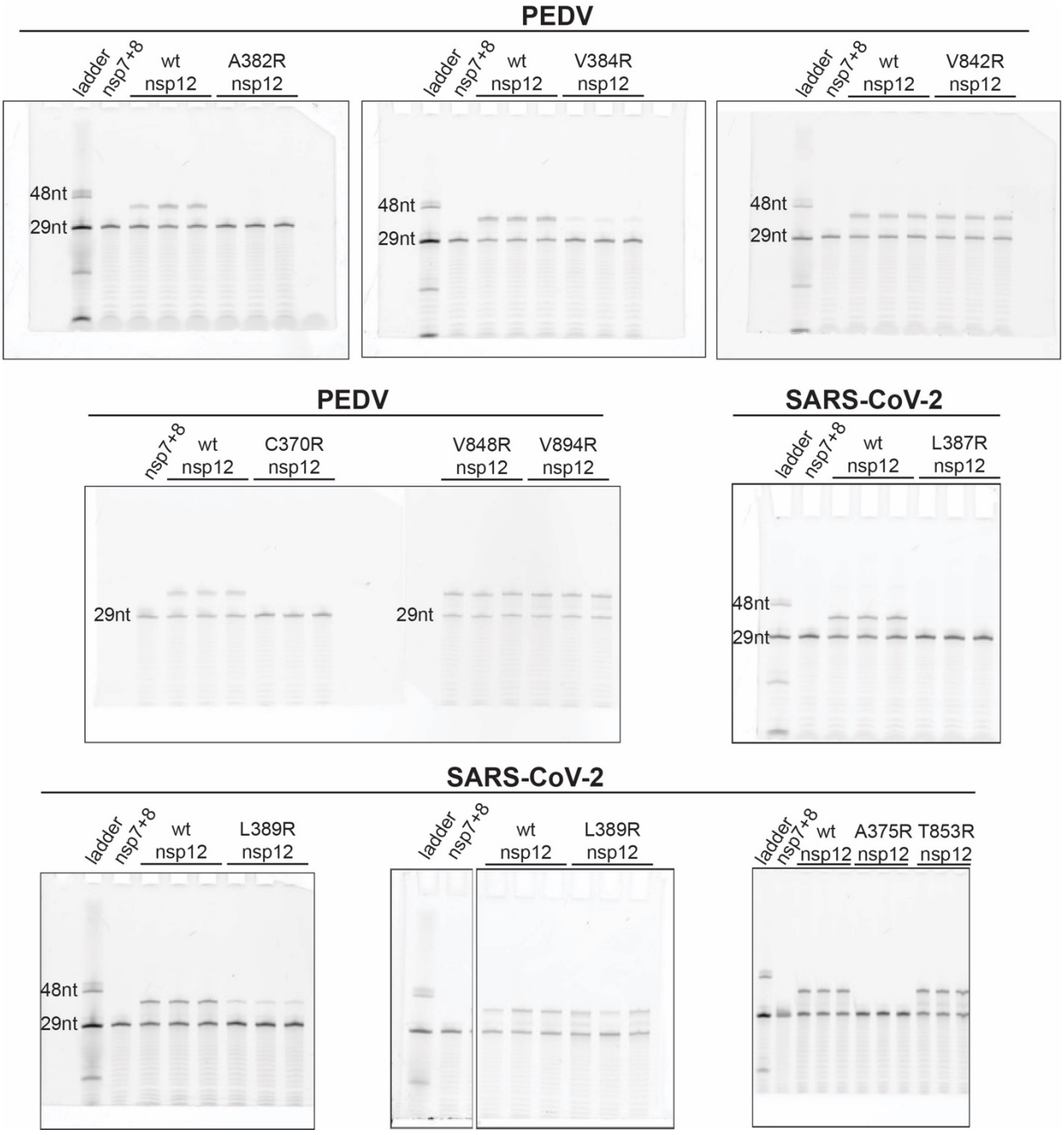

Figure S7, full gel images for mutant nsp12 primer-extension assays: Primer extension results for complexes with mutant nsp12s for PEDV and SARS-CoV-2. For each experiment wildtype (wt) and mutant polymerase reactions were done in triplicate. Viral cofactors, nsp7 and nsp8, were always provided in excess to nsp12 (wt or mutant). Each experiment included one negative control reaction lacking nsp12.

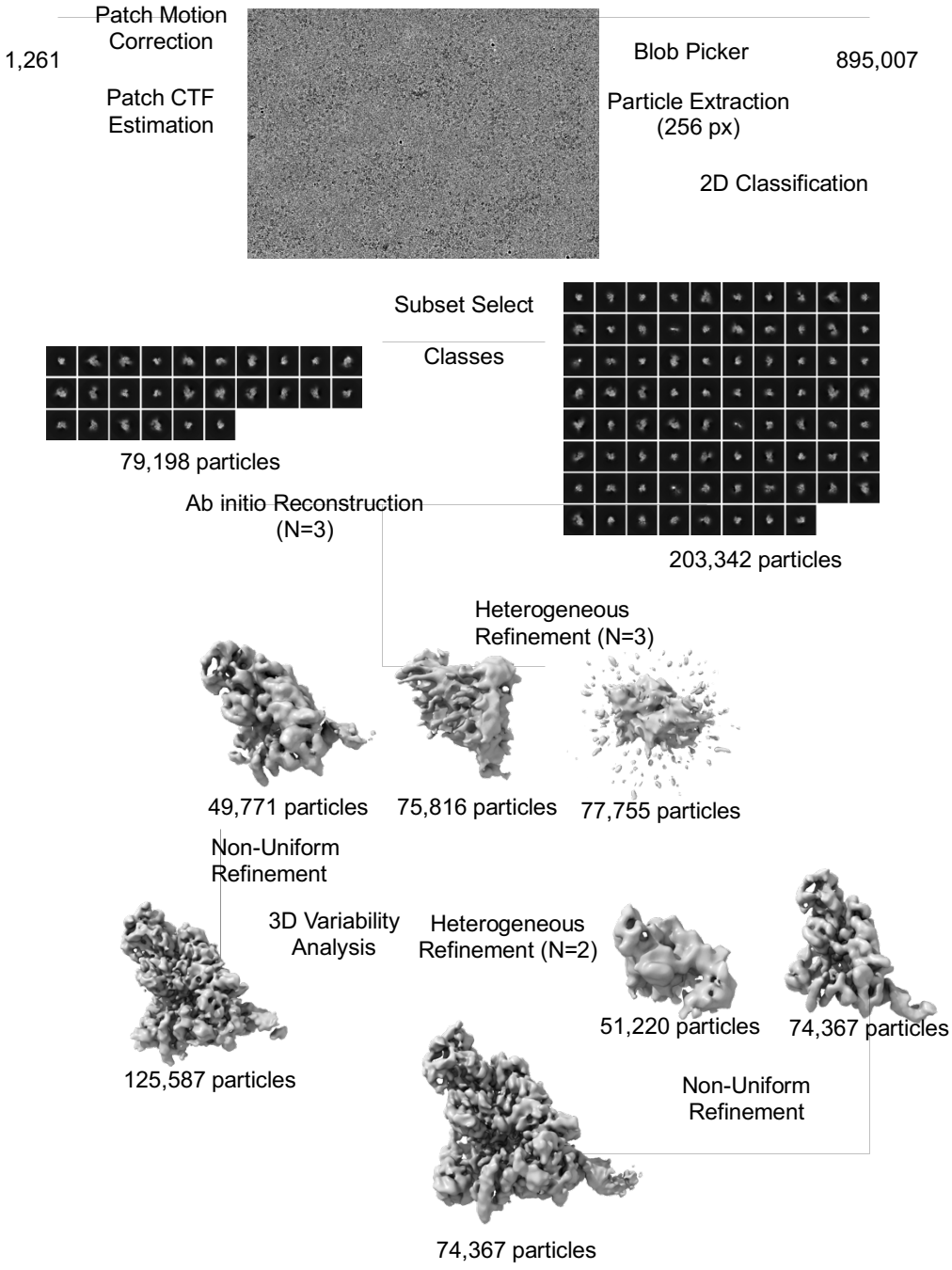

Figure S8, cryo-EM processing pipeline: Workflow for the processing of cryo-EM data starting with 1,261 movies. All data processing was performed in cryoSPARC [1]. Poor particles were removed through multiple rounds of 2D classification, then a subset of polymerase classes were used to generate initial models for subsequent heterogenous refinement with all remaining particles. Particles from classes resembling polymerases were merged for further 3D refinement and a final round of heterogenous refinement into nsp12 alone and polymerase complex maps. The complex map was further refined to our final 3.3 Å reconstruction.

Supplemental References:

1. Punjani, A., et al., *cryoSPARC: algorithms for rapid unsupervised cryo-EM structure determination.* Nat Methods, 2017. **14**: p. 290-296.
2. Sievers, F., et al., *Fast, scalable generation of high-quality protein multiple sequence alignments using Clustal Omega.* Mol Syst Biol, 2011. **7**: p. 539.